Capacitance enhancement in Coulomb blockade tunnel barriers

M. Hofheinz, X. Jehl, and M. Sanquer*
DSM-DRFMC-SPSMS, CEA-Grenoble, 17 rue des Martyrs, 38054 Grenoble Cedex, France

G. Molas, M. Vinet, and S. Deleonibus
DRT-LETI-D2NT-LNDE, CEA-Grenoble, 17 rue des Martyrs, 38054 Grenoble Cedex, France
(Received 12 February 2007; published 1 June 2007)

We study the capacitance of tunnel barriers in well-controlled, very small, silicon single-electron transistors. We observe a decrease of the charging energy of the Coulomb island as the quantum dot is filled from a few to more than 200 electrons. Since the gate capacitance in our devices is, in average, constant all over this electron-density range, we can attribute the observed variation to the source and drain capacitances, made of a doped semiconductor. The capacitance data can be translated into a variation of the electronic polarizability and localization length, in excellent agreement with an independent and simultaneous estimation based on the conductance.

DOI: 10.1103/PhysRevB.75.235301 PACS number(s): 73.23.Hk, 71.30.+h, 72.15.Rn

Capacitance spectroscopy of single-electron tunneling (SET) events has been used from the very beginning of the studies on semiconducting quantum dots, either to probe their discrete energy spectrum[1] or the linewidth of Coulomb blockade peaks.[2–4] Although this primary goal is still very active,[5] recent measurements of the RC relaxation time in the frequency domain showed the importance of combined measurements of conductance and capacitance.[6,7] Most capacitance spectroscopy experiments concentrate on the filling capacitance of quantum dots, which arises from a finite mean energy-level spacing.[6,8] However, this quantum correction always comes in addition to a geometrical capacitance, which arises from the electrostatic coupling to the sourrounding electrodes. In this work, we concentrate on these coupling capacitances which are a property not of the quantum dot but of its surrounding dielectrics. We investigate the relationship between static coupling capacitances and tunnel conductances. Coulomb blockade offers a unique way to measure simultaneously the capacitance and conductance of a tunnel dielectrics. Here, we measure both quantities over a very large range of carrier concentrations in dots, whose surface area remains fixed. We prove that the size does not change by observing a constant gate capacitance. Both capacitance and conductance increase with the carrier's energy, and we give a quantitative model for both quantities over a large range of energy. At high density, cotunneling effects remain weak, which allows a simple interpretation of the data. The analysis of the capacitances of the tunnel barriers is also simplified because our devices have negligible stray capacitances and feature extremely stable electrical characteristics. These properties are specific to our samples which feature a single top gate, a size fixed by lithography, and, being made of silicon, a relatively high density of states. Their design is derived from silicon-on-insulator (SOI) ultrasmall metal-oxide-semiconductor field-effect transistors, adapted in terms of doping to become controlled SET transistors at low temperature.[9] The source and drain are highly doped, while the region below the gate and spacers is lightly doped[10] (As, 5×10^{23} m^{-3}). The quantum dot appears at the overlap between the etched silicon nanowire and the short polysilicon gate, isolated with SiO_2 [Fig. 1(a)]. The surface area of the dot is thus fixed by lithography and can be as small as 3000 nm^2. Our SET transistor can be modeled as a three-capacitor network: the capacitances (called hereafter source and drain capacitances, C_s and C_d) arising from the two SET barriers and the gate capacitance C_g controlling the electrostatic potential on the island. As explained hereafter, the stray capacitances are negligible in our device. Measuring the Coulomb oscillations [Fig. 1(b)] allows one to determine the three capacitances [Fig. 1(c)]. C_g is simply set by the spacing in gate voltage ΔV_g between subsequent peaks, through the relation $C_g=\frac{e}{\Delta V_g}\left(1+\frac{C_\Sigma\Delta_1}{e^2}\right)\simeq e/\Delta V_g$ (e is the electron charge, Δ_1 the mean one-particle level spacing, and $\Delta_1\ll e^2/C_\Sigma$, with

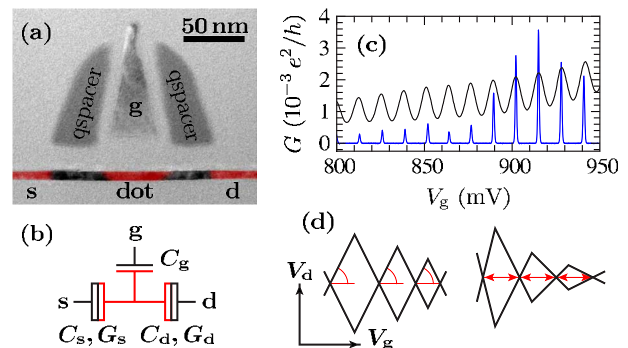

FIG. 1. (Color online) (a) Transmission electron micrograph of a transistor along the source-drain axis. The nanowire is the dark line running below the gate (g) and spacers. In the parts of the wire beyond the spacers and, at positive gate voltage, below the gate, the electron concentration is high enough for the wire to become metallic. These parts form the source (s), dot, and drain (d). (b) Equivalent electrostatic circuit of our samples with the gate capacitance C_g, and the tunnel barriers (boxes) between the Coulomb island (central node) and the source (s) and drain (g). These barriers have tunnel conductances (G_s and G_d), but also capacitances (C_s and C_d). The displacement charge is spread over the three internal capacitor plates. (c) Drain-source conductance G versus gate voltage V_g at 400 mK (bottom curve) and 4.2 K (top curve). (d) Two ways how Coulomb diamonds can fluctuate. Left: variable peak spacing ΔV_g and constant slopes, i.e., constant coupling capacitances and fluctuating filling capacitance e^2/Δ_1. Right: constant peak spacing and variable slopes, i.e., fluctuating C_s and C_d, constant C_g, and negligible Δ_1 (see text).

 ©2007 The American Physical Society

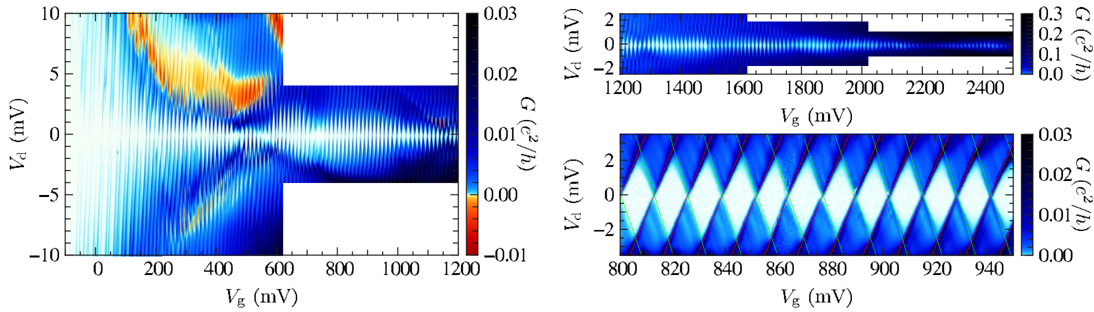

FIG. 2. (Color online) Left and upper right: Coulomb blockade spectroscopy in a $W=60$ nm, $L_g=30$ nm gated nanowire, with the same V_g and V_d scales but different (nonlinear) color scales. Lower right: close-up on a few diamonds showing the fits (lines) allowing one to extract the source and drain capacitances, once the gate capacitance is known.

$C_\Sigma=C_s+C_d+C_g$). C_s and C_d can be determined by studying nonlinear transport through the device. Adding a dc bias to the small ac signal used to probe the source-drain current and plotting this current versus gate and bias voltages result in characteristic diamond-shaped patterns. When the source is grounded and bias is applied to the drain, the positive slope of the diamonds is $1+C_s/C_g$ and the negative slope is $-C_d/C_g$ (see Fig. 2). In the literature, however, this scheme has not been used for capacitance spectroscopy over a large range of electron numbers. Our quantum dot design is ideal for that goal because it has negligible stray capacitances (see inset of Fig. 3), which would dominate the capacitance of the source and drain barriers. Unlike other experiments where stray capacitances can be ten times larger than the capacitances under investigation, here they are at least ten times smaller. For instance, stray capacitances are large in quantum dots formed by depletion gates or for nanotubes or nanowires attached to large metallic pads. Our situation is more similar to vertical quantum dots,[11] where the dot-lead capacitance is dominated by the epitaxially grown tunnel barriers. In our samples, the direct capacitance between dot and ground, in particular, is very reduced (roughly 1 order of magnitude below most GaAs quantum dots) because of the thick buried oxide of the SOI technology combined with small sizes. Unlike when barriers are defined by split gates, here the direct capacitance between the dot and leads is not screened by the large direct capacitive coupling to the gates.[8]

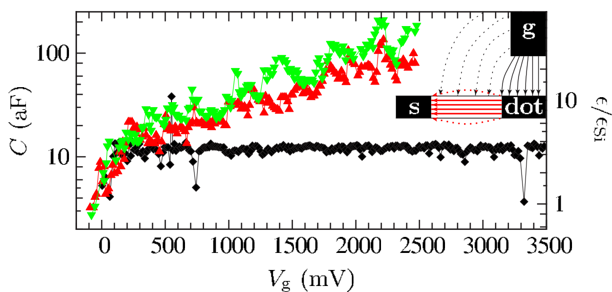

FIG. 3. (Color online) Gate (♦), source (▲), and drain (▼) capacitances extracted from the Coulomb blockade diamonds shown in Fig. 2. The gate capacitance is constant because the size of the dot is fixed. The right scale indicates the dielectric constant in the source and drain capacitors. The inset illustrates the main contributions to the capacitances: The border effects in the source-dot capacitor (dotted horizontal electric field lines) can be neglected despite its long aspect ratio because $\epsilon_{\text{barrier}} \gg \epsilon_{SiO_2}, \epsilon_{Si_3N_4}$. This fact is confirmed by the good agreement between $\epsilon_{\text{barrier}}$ and ϵ_{Si} at $V_g=0$ V, where the contribution of the donors to the dielectric constant is weak.

As our devices are cooled down below approximately 20 K, the smooth transistorlike characteristics are replaced by periodic and reproducible oscillations [Fig. 1(b)]. The period is set only by the geometry of the overlap between the nanowire and the gate.[9,12] Fluctuations around the mean period are very small, of the order of the mean energy-level spacing Δ_1. Δ_1 and the quantum correction to the capacitance are small (except for the first electrons).[13,14] Coulomb diamonds measured at 400 mK are shown in Fig. 2. Such time-consuming recording is possible and relevant only in devices with very high immunity to environmental charge noise. Although Coulomb diamonds have already been analyzed thoroughly, typically for the first tens of electrons,[11,15] to our knowledge, clear Coulomb blockade diamonds have not yet been shown over a range of more than $N=200$ electrons.

The gate, source, and drain capacitances extracted from our data are shown in Fig. 3. The fact that C_g (obtained from the peak spacing) does not change with gate voltage is not surprising, since the size of the dot is set by lithography. However, this unique property is crucial for interpreting the general behavior of Fig. 2. As expected, the charging energy (height of the diamonds) decreases as N increases. In most experiments, C_g varies but the slopes are roughly the same from one diamond to the other.[11,15] Our data exhibit a different behavior: the slopes of the diamonds vary significantly with V_g, whereas the peak spacing (C_g) remains constant [Fig. 1(d)]. This necessarily implies a variation of C_s and C_d. As shown in Fig. 3, we observe a net increase of C_s and C_d by a factor of 30. Both the initial value at $V_g \approx 0$ and the enhancement with V_g can be understood by taking into account the microscopic properties of our tunnel barriers.

Our measurement probes the two capacitors between the channel of the transistor and the highly doped, metalliclike, source and drain. The dielectrics are short sections of low-doped silicon, below the spacers. In undoped Si, the dielectric constant ϵ_{Si} and the associated geometric capacitance are set by the band gap.[16] In doped silicon, there is a finite density of localized states at the Fermi level, whose polarizability ϵ can be large ($\approx 10^{-35}$ F m^2 for dilute As donors[17]) and is known to diverge as the Fermi energy approaches the mobility edge from the bottom.[18,19] Indeed, Imry *et al.*[19] suggested that

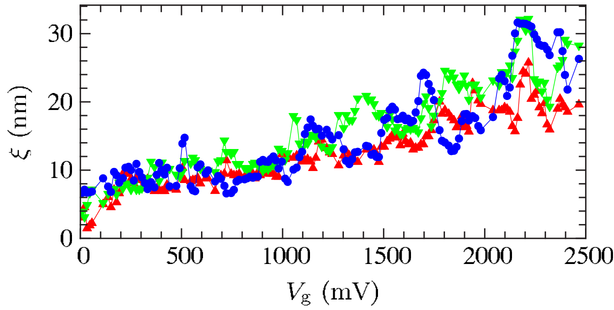

FIG. 4. (Color online) Localization length versus gate voltage obtained from source capacitance (▲), drain capacitance (▼), and conductance (●), supposing equal source and drain transparencies. The fitting parameters, $g_0=5e^2/h$ and $\beta\lambda^{-2}=0.05\ \text{nm}^{-2}$, are global for all samples with the same doping and spacer widths. The value of ξ is comparable to the Bohr radius at low gate voltage and to the thickness of the barrier (35 nm) at high gate voltage.

$$\epsilon = \epsilon_0\epsilon_{\text{Si}} + \beta e^2 N(E_F)\xi^2 = \epsilon_0\epsilon_{\text{Si}} + \beta\frac{\xi^2}{\lambda^2}, \tag{1}$$

where $\epsilon_{\text{Si}}=11.9$ is the static dielectric constant, far in the insulating regime, and λ is the Thomas-Fermi screening length. β is a model-dependent numeric constant of order unity.[20] In bulk doped silicon, the localization length ξ, which characterizes the spatial extension of the carrier wave functions, diverges at a critical doping concentration ($6.4\times10^{24}\ \text{m}^{-3}$ for Si:As).[18] In our nanoscopic capacitor, the divergence of ξ is limited by the capacitor length L at large V_g. ξ not only determines the polarizabity but also the transparency of the dielectrics. In fact, the tunnel conductance g in units of $\frac{e^2}{h}$ of a disordered dielectric is given by

$$\langle \ln g\rangle = \frac{-2L}{\xi} + \ln g_0, \tag{2}$$

valid for $\xi \ll L$ (i.e., $g \ll 1$).[21,22] ξ is of the order of the Bohr radius (3.3 nm) for energies well below the mobility edge, in the limit of diluted, isolated donors, and increases with energy when wave functions on separate donors begin to overlap. g_0 is close to unity. $\xi \leqslant L$ means that (i) the conductance is smaller than the quantum, a prerequisite for observing Coulomb blockade accross the dielectrics, and (ii) the conductance is an exponential function of the length.

These remarkably simple results [Eqs. (1) and (2)] are obtained after averaging over disorder configurations despite the complexity brought by disorder and interactions. Due to their small volume and thanks to Coulomb blockade, our samples provide a way of measuring simultaneously the dc conductance and capacitance of a coherent doped semiconductor, and testing if a single parameter (ξ) is enough to explain the mean behavior of both polarizability and transparency.

Figure 4 shows ξ obtained from capacitance and conductance as a function of gate voltage. In order to determine ξ from the source or drain capacitances, we first identify the increase of the capacitance as an increase of the dielectric constant for a fixed geometry. Then we apply Eq. (1) with $\beta\lambda^{-2}=0.05\ \text{nm}^{-2}$, the first fitting parameter. With β from Ref. 20, this corresponds to $\lambda=14$ nm, a value close to the average distance between As donors[10] implanted at $5\times10^{23}\ \text{m}^{-3}$. In order to extract the dielectric constant from the source and drain capacitances, we consider the planar capacitor formed by the dot on one side and the reservoirs on the other. The surface of the plates is the cross section of the wire, $40\times17\ \text{nm}^2$. The distance between the plates is $L=35$ nm, the distance between the heavily doped source (drain) and the accumulation dot (see inset of Fig. 3). It is defined by the width of the spacers. We neglect the border effect because $\epsilon_{\text{Si}}=11.9$ is much larger than in surrounding silica ($\epsilon_{\text{SiO}_2}=3.9$). The heavily doped source electrode is not modified by the gate voltage. We can also neglect the lateral increase of the dot size (which would result in a decrease of L) because the gate capacitance is constant. The extension of the dot as a function of V_g could only change perpendicularly to the wire. We suppose the dot to occupy the full wire cross section. In other words, we suppose the density of carriers to be constant over the thickness. With this hypothesis, we obtain a very good agreement with the dielectric constant for pure silicon at low gate voltage (see right scale of Fig. 3).

In order to determine ξ from the conductance, we suppose that the source and drain tunnel conductances are equal $g_s=g_d$, which is valid in average. Within the orthodox model for Coulomb blockade, i.e., for $\Delta_1 \ll k_BT$, the drain-source conductance on top of the Coulomb resonances is then given by

$$g_{\max} = \frac{1}{2}\frac{g_s g_d}{g_s+g_d} = \frac{g_s}{4}. \tag{3}$$

ξ is then calculated via Eq. (2) for $g_s=g_d$ with $g_0=5\frac{e^2}{h}$, a second fitting parameter. The two fitting parameters are not chosen individually for each sample but adjusted globally for all samples with the same doping profile but different wire cross sections.

Figure 4 shows the excellent agreement for the values of ξ obtained from conductance and capacitance, even though ξ varies by a factor of more than 5. Such a variation corresponds to an increase by a factor of 30 in capacitance and an increase by 2 orders of magnitude in the tunnel current. Note that Eq. (2) does not contain the density of states explicitly, which reflects the dominance of a single channel on the conductance of a disordered dielectrics.

The large fluctuations around the mean monotonic increase on Fig. 4 reflect the fluctuations of the measured conductance and capacitance of our doped dielectrics. As usual in mesoscopic quantum physics, the microscopic or macroscopic parameters (density of states, diffusion constant, shape, and dimensionality), which are summarized in a single quantity ξ, are not enough to determine the actual conductance and capacitance of a particular sample. Lognormal fluctuations of the conductance are expected in a mesoscopic disordered dielectrics whether it is quantum coherent[23] or not,[22] and especially in a lightly doped semiconductor nanowire. Again, these fluctuations (comparable to the mean value) reflect the dominance of a single conducting channel, which changes with energy or gate voltage.[24] In our study, mesoscopic fluctuations of the dielectric constant

are observed (see Fig. 3). Unfortunately, there exists no theoretical estimation for these capacitance fluctuations for a quantum coherent dielectrics, unlike for the conductance. Nevertheless, the observed fluctuations of the capacitance are found to be comparable in amplitude with the observed fluctuations of conductance, once translated in terms of localization length variation with Eqs. (1) and (2). In our very small doped dielectrics, mesoscopic fluctuations of the dielectric constant are comparable to the mean value. Such large fluctuations are expected in classical Coulomb glass, where the wave-function overlap between localized states is neglected.[25] More studies are required to distinguish between classical and quantum effects.

A measurement of both the polarizability and the conductance of a mesoscopic insulator has been performed on the same system. Coulomb blockade in an original single-electron transistor design with very low stray capacitances and well-defined geometry has allowed one to access both quantities. We have found that, despite strong interactions, a single parameter, the localization length ξ, can accurately describe both the evolution of the polarizability and the conductance. The good agreement as well as the strong fluctuations indicate that not only the conductance but also the polarizability is dominated by one or few localized states.

This work was partly supported by the European Commission under the frame of the Network of Excellence "SiNANO" (No. IST-506844).

*Electronic address: marc.sanquer@cea.fr

[1] R. C. Ashoori, H. L. Stormer, J. S. Weiner, L. N. Pfeiffer, S. J. Pearton, K. W. Baldwin, and K. W. West, Phys. Rev. Lett. **68**, 3088 (1992).

[2] K. A. Matveev, Phys. Rev. B **51**, 1743 (1995).

[3] L. W. Molenkamp, K. Flensberg, and M. Kemerink, Phys. Rev. Lett. **75**, 4282 (1992).

[4] D. Berman, N. B. Zhitenev, R. C. Ashoori, and M. Shayegan, Phys. Rev. Lett. **82**, 161 (1999).

[5] S. Ilani, L. A. K. Donev, M. Kindermann, and P. L. McEuen, Nat. Phys. **2**, 687 (2006).

[6] M. Büttiker, A. Prêtre, and H. Thomas, Phys. Rev. Lett. **70**, 4114 (1993).

[7] J. Gabelli, G. Fève, J.-M. Berroir, B. Placais, A. Cavanna, B. Etienne, Y. Jin, and D. C. Glattli, Science **313**, 499 (2006).

[8] T. Christen and M. Büttiker, Phys. Rev. Lett. **77**, 143 (1996).

[9] M. Hofheinz, X. Jehl, M. Sanquer, G. Molas, M. Vinet, and S. Deleonibus, Appl. Phys. Lett. **89**, 143504 (2006).

[10] M. Hofheinz, X. Jehl, M. Sanquer, M. Vinet, B. Previtali, D. Fraboulet, D. Mariolle, and S. Deleonibus, Eur. Phys. J. B **54**, 299 (2006).

[11] S. Tarucha, D. G. Austing, T. Honda, R. J. van der Hage, and L. P. Kouwenhoven, Phys. Rev. Lett. **77**, 3613 (1996).

[12] M. Hofheinz, Ph.D. thesis, Université J. Fourier.

[13] M. Boehm, M. Hofheinz, X. Jehl, M. Sanquer, M. Vinet, B. Previtali, D. Fraboulet, D. Mariolle, and S. Deleonibus, Phys. Rev. B **71**, 033305 (2005).

[14] At $V_g \leqslant 0$, i.e., for the first peaks, Δ_1 is not negligible. Although it certainly deserves more attention, we do not focus on the case of few electrons in the present study on a large electron density range.

[15] M. T. Björk, C. Thelander, A. E. Hansen, L. E. Jensen, M. W. Larsson, L. R. Wallenberg, and L. Samuelson, Nano Lett. **4**, 1621 (2004).

[16] J. M. Ziman, *Principles of the Theory of Solids* (Cambridge University Press, Cambridge, 1964).

[17] T. G. Castner, Phys. Rev. B **21**, 3523 (1980).

[18] T. G. Castner, N. K. Lee, G. S. Cieloszyk, and G. L. Salinger, Phys. Rev. Lett. **34**, 1627 (1975).

[19] Y. Imry, Y. Gefen, and D. J. Bergman, Phys. Rev. B **26**, 3436 (1982).

[20] Efetov's value is $\beta = 8\zeta(3) \simeq 9.62$ (after conversion to SI units and multiplication by π); see K. Efetov, *Supersymmetry in Disorder and Chaos* (Cambridge University Press, Cambridge, 1997).

[21] A. D. Mirlin, Phys. Rep. **326**, 249 (2000).

[22] M. E. Raikh and I. M. Ruzin, in *Mesoscopic Phenomena in Solids*, edited by B. L. Altshuler, P. A. Lee, and R. A. Webb (Elsevier, Amsterdam, 1991).

[23] A. D. Stone, P. A. Mello, K. A. Muttalib, and J. L. Pichard, *Mesoscopic Phenomena in Solids*, edited by B. L. Altshuler, P. A. Lee, and R. A. Webb (Elsevier, Amsterdam, 1991).

[24] A. B. Fowler, A. Hartstein, and R. A. Webb, Phys. Rev. Lett. **48**, 196 (1982); A. B. Fowler, J. J. Wainer, and R. A. Webb, IBM J. Res. Dev. **32**, 372 (1988); R. J. F. Hughes, A. K. Savchenko, J. E. F. Frost, E. H. Linfield, J. T. Nicholls, M. Pepper, E. Kogan, and M. Kaveh, Phys. Rev. B **54**, 2091 (1996); W. Poirier, D. Mailly, and M. Sanquer, *ibid.* **59**, 10856 (1999).

[25] A. A. Koulakov, F. G. Pikus, and B. I. Shklovskii, Phys. Rev. B **55**, 9223 (1997).